NASA / TM—1999-208837

Common-Path Phase-Stepped Interferometer for Fluid Measurements

Carolyn R. Mercer
Glenn Research Center, Cleveland, Ohio

Nasser Rashidnia
National Center for Microgravity Research, Cleveland, Ohio

September 1999

The NASA STI Program Office . . . in Profile

Since its founding, NASA has been dedicated to the advancement of aeronautics and space science. The NASA Scientific and Technical Information (STI) Program Office plays a key part in helping NASA maintain this important role.

The NASA STI Program Office is operated by Langley Research Center, the Lead Center for NASA's scientific and technical information. The NASA STI Program Office provides access to the NASA STI Database, the largest collection of aeronautical and space science STI in the world. The Program Office is also NASA's institutional mechanism for disseminating the results of its research and development activities. These results are published by NASA in the NASA STI Report Series, which includes the following report types:

- TECHNICAL PUBLICATION. Reports of completed research or a major significant phase of research that present the results of NASA programs and include extensive data or theoretical analysis. Includes compilations of significant scientific and technical data and information deemed to be of continuing reference value. NASA's counterpart of peer-reviewed formal professional papers but has less stringent limitations on manuscript length and extent of graphic presentations.

- TECHNICAL MEMORANDUM. Scientific and technical findings that are preliminary or of specialized interest, e.g., quick release reports, working papers, and bibliographies that contain minimal annotation. Does not contain extensive analysis.

- CONTRACTOR REPORT. Scientific and technical findings by NASA-sponsored contractors and grantees.

- CONFERENCE PUBLICATION. Collected papers from scientific and technical conferences, symposia, seminars, or other meetings sponsored or cosponsored by NASA.

- SPECIAL PUBLICATION. Scientific, technical, or historical information from NASA programs, projects, and missions, often concerned with subjects having substantial public interest.

- TECHNICAL TRANSLATION. English-language translations of foreign scientific and technical material pertinent to NASA's mission.

Specialized services that complement the STI Program Office's diverse offerings include creating custom thesauri, building customized data bases, organizing and publishing research results . . . even providing videos.

For more information about the NASA STI Program Office, see the following:

- Access the NASA STI Program Home Page at ***http://www.sti.nasa.gov***

- E-mail your question via the Internet to help@sti.nasa.gov

- Fax your question to the NASA Access Help Desk at (301) 621-0134

- Telephone the NASA Access Help Desk at (301) 621-0390

- Write to:
  NASA Access Help Desk
  NASA Center for AeroSpace Information
  7121 Standard Drive
  Hanover, MD 21076

NASA / TM—1999-208837

Common-Path Phase-Stepped Interferometer for Fluid Measurements

Carolyn R. Mercer
Glenn Research Center, Cleveland, Ohio

Nasser Rashidnia
National Center for Microgravity Research, Cleveland, Ohio

Prepared for the
Eighth International Symposium on Flow Visualization
sponsored by the International Flow Visualization Society
Sorrento, Italy, September 1–4, 1998

National Aeronautics and
Space Administration

Glenn Research Center

September 1999

Available from

NASA Center for Aerospace Information
7121 Standard Drive
Hanover, MD 21076
Price Code: A03

National Technical Information Service
5285 Port Royal Road
Springfield, VA 22100
Price Code: A03

COMMON-PATH PHASE-STEPPED INTERFEROMETER FOR FLUID MEASUREMENTS

Carolyn R. Mercer
National Aeronautics and Space Administration
Glenn Research Center
Cleveland, Ohio 44135

Nasser Rashidnia
National Center for Microgravity Research
NASA Glenn Research Center
Cleveland, Ohio 44135

Abstract

The liquid-crystal point-diffraction interferometer is a new phase-stepped, common-path interferometer. A microsphere in a liquid crystal layer is used to locally generate a reference beam and phase-shift the object beam. The result is an interferometer that provides quantitative, high-density data in relatively high vibration environments. This paper describes a comparison between the liquid-crystal PDI and a phase-stepped Mach-Zehnder interferometer. Both were used to simultaneously measure temperature distributions in an oil bath. Very good agreement between the data from both interferometers is shown, and the common-path interferometer is shown to be more robust in the presence of vibrations.

1. Introduction

Common-path interferometers have a large advantage over conventional split path interferometers because they are less sensitive to environmental vibration and temperature disturbances. This feature is highly desirable in aerospace applications where the object of interest is often a supersonic, noisy, gas flow. In the last decade phase shifting interferometry has become the standard way to extract numerical information from interferograms. However, it is not trivial to incorporate phase shifting into common-path interferometers because of the difficulty in modifying one beam and not the other. This difficulty is in fact the source of the common-path interferometer's robustness.

The liquid crystal point diffraction interferometer was invented to solve this problem of incorporating phase stepping capability into a common path interferometer. The device is described in detail in Ref. 1 and shown in Figure 1. Briefly, a 9-micron layer of dyed, nematic liquid crystals is sandwiched between two glass plates, each coated with a transparent ITO electrode. 9-micron diameter microspheres are embedded in the liquid crystal layer. A collimated laser beam is transmitted through the object of interest, encoding refractive index disturbances into the beam's wavefront. This beam is focused onto one microsphere such that the beam waist is larger than the microsphere.

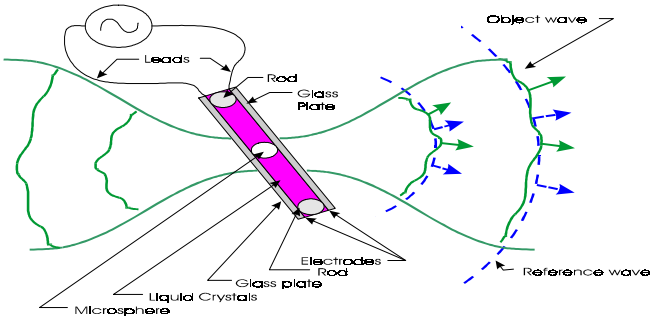

Fig. 1. Schematic of liquid crystal PDI.

The microsphere serves as a spatial filter, forming a spherical reference wave by diffraction. The portion of the object beam that passes around the microsphere travels through the liquid crystals and retains its object information. Dye is added to the liquid crystals to equalize the amplitudes of the object and reference beams. The object and locally generated reference beams diverge coincidentally, forming an interferogram on a detector. The phase of the object beam is stepped by successively incrementing the amplitude of an AC voltage applied across the electrodes. Voltages ranging from 460 to 650 mV rms are used to produce five ninety-degree phase steps. The interferograms are digitized and processed to produce line-of-sight integrals of the optical path length distribution of the object under study. If the physical path length is constant from frame-to-frame, then the refractive index distribution is measured. Conversely, if the refractive index is constant the physical path length is measured. This paper describes the former case.

The accuracy of the LCPDI has been verified by comparing its data to traversing thermocouple data.[2] The data showed good agreement, but the thermocouple had coarse temperature resolution. An experiment was therefore set up to compare measurements made with the LCPDI to the same measurements made with a conventional interferometer. A Mach-Zehnder interferometer was chosen as the comparison instrument because of its widespread use, particularly in aerospace applications.[3] This paper describes the experimental apparatus for simultaneous temperature measurements, the data reduction process and results, a comparison of the two interferometers in a vibrating environment, and conclusions based on the results.

2.0 Comparison of LCPDI and Mach-Zehnder interferometers

2.1 Experimental equipment

The experimental configuration for the comparison between the Mach-Zehnder and LCPDI is shown in Figure 2. A horizontally polarized, diode-pumped frequency doubled YAG laser was attenuated to 5mW by neutral density filter ND, then expanded and collimated by EXPND to produce a 47mm diameter beam. Beamsplitter BS1 creates the reference beam for the Mach-Zehnder. Mirror M2 in this reference arm is mounted on a piezoelectrically driven stage to provide phase control for the Mach-Zehnder. The object beam reflects off of mirror M3 and passes through optical windows in a 38x19x18 mm rectangular oil-filled chamber with recirculating water flowing through the top and bottom walls for temperature control. Aperture AP limits the field of view to 12.35 mm and horizontal linear polarizer LP blocks vertically polarized scattered light. Beamsplitter BS2 samples off 50% of the object beam for the LCPDI. The remainder of the object beam hits beamsplitter BS3 which recombines it with the reference beam on Camera CAM2. The light reflected off of BS2 is focused by a 100mm f/2.8 Cooke triplet lens L1 to a point just before the LCPDI. The interferogram created by the LCPDI

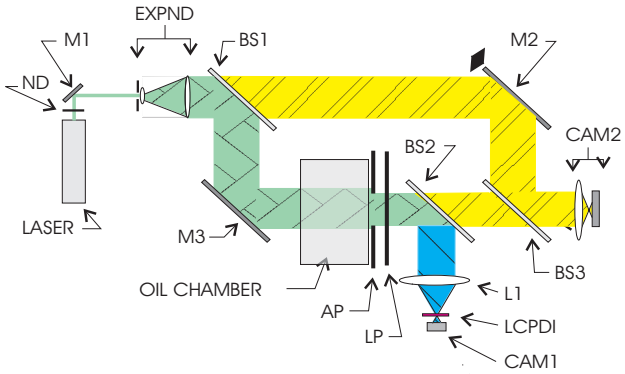

Fig. 2. Simultaneous measurement using LCPDI (blue, signal-hatched) and Mach-Zehnder (yellow, double hatched) interferometers. Beams common to both are indicated in green cross-hatching.

is recorded by CCD array CAM1. The recorded interferograms from both cameras are digitized by frame grabbers in a Pentium computer. The computer controls the piezoelectric driver for mirror M2, the voltage across the LCPDI, and the frame grabbers. Interferograms from the LCPDI and the Mach-Zehnder were recorded within $1/30^{th}$ second of each other.

The temperature of the top wall of the oil filled chamber was set to 24 °C. The temperature of the bottom surface of the chamber was varied to measure several temperature distributions. First the bottom was set to 24.6 °C and the chamber was allowed to equilibrate. Five phase-stepped interferograms were recorded with both interferometers; the timing sequence is shown in Figure 3. These interferograms were then stored to disk, and the bottom temperature was reset for the next sequence. Five data sets were collected with the bottom wall temperature set, in turn, to $Tbottom_i$ = 24.6, 23.4, 22.9, 22.0, and 21.6 °C. Finally, the bottom temperature was set to 24.0 °C and five frames were again recorded using both interferograms. This final data set was used as the isothermal reference set.

2.2 Data reduction and results

Each interferogram from the LCPDI was normalized by fitting a 2D Gaussian intensity distribution to it, then taking the ratio of the interferogram to its Gaussian distribution.[1] This was required because the dye used to attenuate the object beam was not rotationally symmetric, causing unwanted amplitude variations when the applied electric field strength was stepped. The normalized LCPDI interferograms and the Mach-Zehnder interferograms were then converted to phase maps using Hariharan's algorithm[4], and the phase was unwrapped by searching rows and columns for discontinuities greater than π radians, then adding the correct multiple of 2π. Each phase map was resized to force both interferometers to have the same pixel resolution; both cameras recorded the same aperture so the pixel scale was determined by counting the number of pixels across the aperture horizontally and vertically for both cameras. The resultant phase maps were 640 x 523 pixels, with a resolution of 0.026 mm/pixel in each dimension. The LCPDI data was then flipped to compensate for the image inversion behind the LCPDI filter.

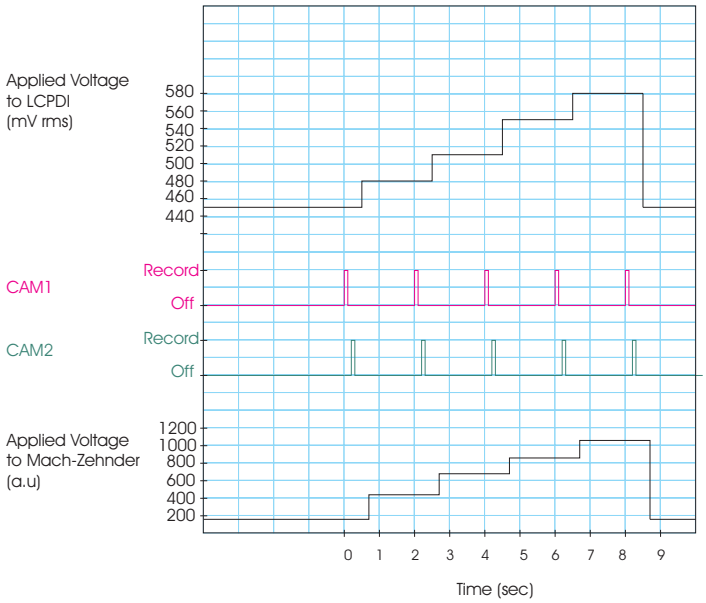

Fig. 3. Data acquisition timing diagram. Sequence is begun (Time t=0) after oil chamber has reached thermal equilibrium

The phase distributions were converted to temperature by:

$$T(x,y) = \phi(x,y)\frac{\lambda}{L\left(dn/dT\right)} \quad (1)$$

where $\phi(x,y)$ is the measured phase at pixel (x,y), the optical wavelength λ = 532 nm, the line-of-sight length of the oil chamber L = 19.0 mm, and dn/dT is given by:[5]

$$dn/dT = \frac{-1.5n\left(n^2-1\right)\beta}{2n^2+1} \quad (2)$$

where the refractive index n = 1.4022 at 25 °C and the coefficient of thermal expansion β = 0.00104 cc/(cc °C) for the 50cs silicone oil that was used. The isothermal temperature distribution $T_{isothermal}(x,y)$ was first computed. The temperature distributions $T_i(x,y)$ for each of the five different bottom surface temperatures were then computed, and the isothermal distribution was subtracted from each to produce a temperature difference maps for each condition:

$$\Delta T_i(x,y) = T_i(x,y) - T_{isothermal}(x,y) \quad (3)$$

Since interferometers measure relative temperature, the temperature at the center pixel of each data set was forced to equal a specific value to permit comparisons between the two interferometers. Since the temperature distribution was assumed to be nominally linear from top to bottom, the center temperature was set to the average of the top and bottom wall temperatures. The value required to ensure this condition was added uniformly to each pixel in a single distribution as follows:

$$\overline{\Delta T_i}(x,y) = \Delta T_i - \Delta T_i(cx,cy) + \frac{\left(Ttop + Tbottom_i\right)}{2} \quad (4)$$

where the center pixel values *cx* and *cy* equal 343 and 267, respectively. Note that the data processing included no spatial filtering.

Temperature maps processed in this way are shown in Figure 4. The top surface of the chamber was set to 24 °C and the bottom was set to 21.6 °C. The data is shown sub-sampled every 5 pixels for clarity. Figure 4a shows the temperature distribution measured with the LCPDI; Figure 4b shows the same data measured with the Mach-Zehnder interferometer. The results are very similar. Figure 5 shows cross sections taken through the center of this data with no sub-sampling, and also through the data taken at the other four bottom temperature settings. The solid lines show data taken with the LCPDI, and the dashed lines are from the Mach-Zehnder. Figure 5a shows vertical cross sections and Figure 5b shows horizontal cross sections, all taken through the center of the aperture. The four data sets obtained with $T_{bottom} < T_{Top}$ show nominally linear temperature distributions from top to bottom. The case where $T_{bottom} > T_{Top}$ shows a slightly curved vertical cross section, indicating the onset of recirculating flow caused by the thermal inversion. In order to compare the two interferometers, a straight line was fit to each curve. The slopes of each of these lines are tabulated in Table 1. Note that the slopes of the lines do not equal the simple expression $(T_{Top} - T_{bottom})/cell\ height$ because the uninsulated chamber had some minor conductive losses from each wall. The difference between the measured total temperature excursions across the aperture for each case is listed in column 4, and the percentage disagreement between the two interferometers is listed in column 5. The vertical slopes listed in Table 1a show agreement within 3.6% for three cases, but relatively large disagreement for the other two cases. The horizontal gradients listed in Table 1b should all be zero. The measured gradients are very small, and in each case the absolute value of the LCPDI-measured gradients are smaller than those measured by the Mach-Zehnder. The same two data sets that showed the largest disagreement in Table 1a show the largest deviation from the expected zero gradient in the horizontal direction.

These two anomalous data sets were taken within 20 minutes of each other but over 4 hours earlier than the isothermal reference data set; the other three data sets were taken within 2 hours of the reference data. A mechanical drift of BS1, BS2, or M3 could explain the observed discrepancies. Slight slope mismatches may also be caused by a rotational misalignment of CAM1 relative to CAM2, but this would cause a constant difference across all data sets. Note also that the LCPDI data is slightly nosier than the Mach-Zehnder data. This can be seen by close inspection of Figure 5, and also in the cross sectional plots. This noise is caused primarily by interference with neighboring microspheres in the LCPDI filter.

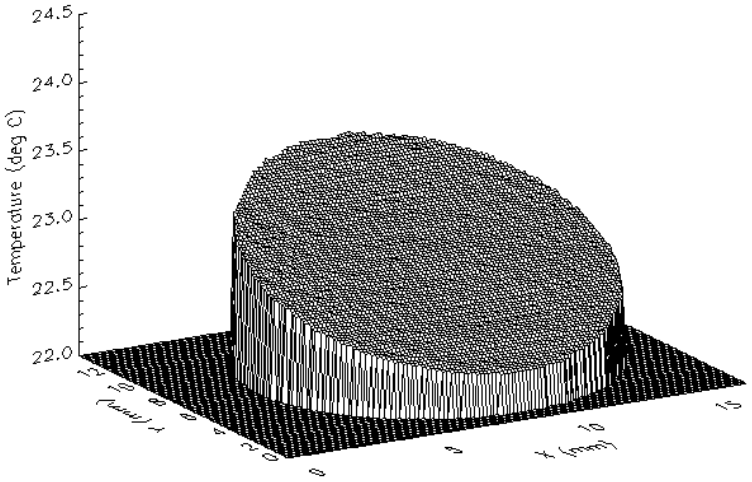

Fig. 4a. Temperature distribution measured with the liquid crystal point diffraction interferometer. Top surface set to 24 C, bottom surface set to 21.6 °C. Data shown is sub-sampled every 5th pixel for clarity.

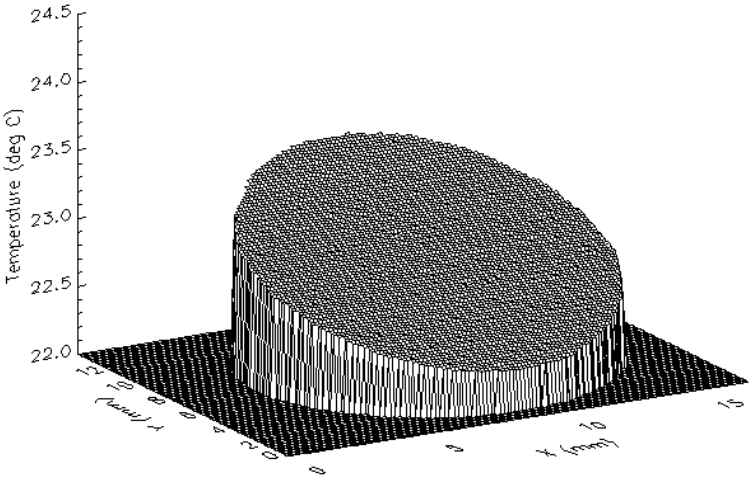

Fig. 4b. Temperature distribution measured with the Mach-Zehnder interferometer. Top surface set to 24 °C, bottom surface set to 21.6 °C. Data shown is sub-sampled every 5th pixel for clarity.

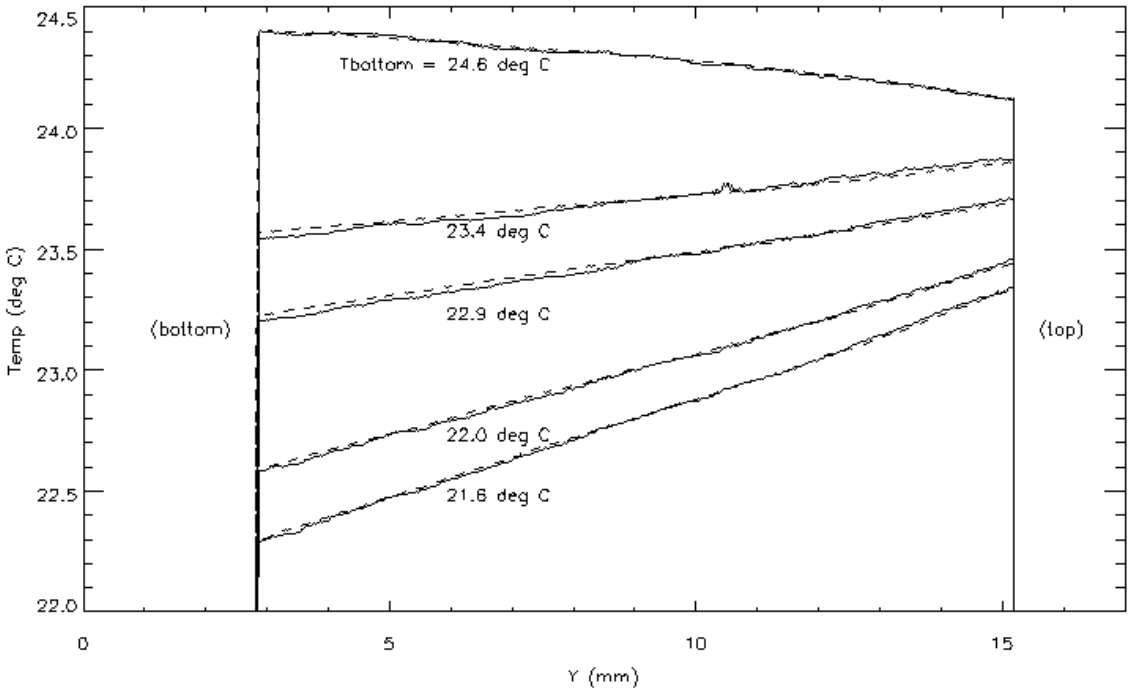

Fig. 5a. Temperature across vertical centerline of cell measured simultaneously with the LCPDI (solid lines) and Mach-Zehnder (dashed lines) interferometers. Top chamber temperature set to 24 °C; bottom temperature set as indicated.

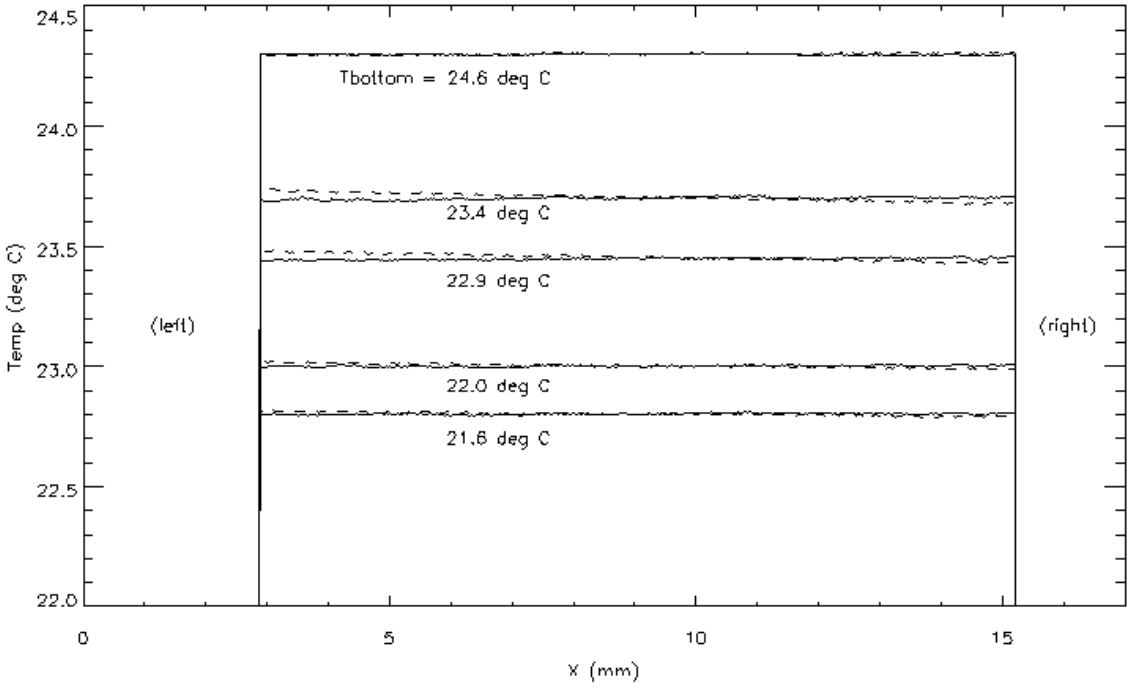

Fig. 5b. Temperature across horizontal centerline of cell measured simultaneously with the LCPDI (solid lines) and Mach-Zehnder (dashed lines) interferometers. Top chamber temperature set to 24 °C; bottom temperature set as indicated.

Tbottom (°C)	Measured dT/dY (°C/mm)		Difference in measured ΔT across 12.35 mm aperture	% difference
	LCPDI	Mach-Zehnder	(°C)	
24.6	-0.0230	-0.0222	0.01	-3.6
23.4	0.0273	0.0229	-0.05	-19.2
22.9	0.0409	0.0370	-0.05	-10.5
22.0	0.0701	0.0679	-0.03	-3.2
21.6	0.0850	0.0829	-0.02	-2.5

Table 1a.—Vertical thermal gradients measured with LCPDI and Mach-Zehnder at five temperature settings with the top surface temperature set to 24.0 °C. The third column shows the difference between the two interferometers in measuring the change in temperature from bottom to top; $(dT/dY_{MZ} - dT/dY_{LCPDI})*12.35mm$, and the fourth column shows the percent difference between the slopes measured by the two instruments.

Tbottom (°C)	Measured dT/dX (°C/mm)		Difference in measured ΔT across 12.35 mm aperture
	LCPDI	Mach-Zehnder	(°C)
24.6	-0.0003	0.0008	0.01
23.4	0.0011	-0.0044	-0.04
22.9	0.0009	-0.0040	-0.04
22.0	0.0005	-0.0022	-0.03
21.6	0.0004	-0.0018	-0.03

Table 1b.—Horizontal thermal gradients measured with LCPDI and Mach-Zehnder at five temperature settings with the top surface temperature set to 24.0 °C. The third column shows the difference between the two interferometers in measuring the change in temperature from left to right; $(dT/dX_{MZ} - dT/dX_{LCPDI})*12.35mm$.

2.3 Vibration testing

The oil chamber was removed from the optical path and interferograms from the LCPDI and Mach-Zehnder interferometers were recorded. Typical interferograms are shown in Figure 6 (a) and (b). Although both interferograms are recording the same object (room air), they appear different because the LCPDI interferogram has defocus fringes and the Mach-Zehnder has tilt fringes. This difference is not significant because these background patterns are subtracted out during data processing (Eqn. 3). The table upon which all of the optics shown in Figure 2 were mounted was then vibrated at 6 Hz. An acceleration of 3.2 mG was measured at a point on the table surface near the two cameras and the interferograms were recorded again. This very low amplitude vibration completely washed out the Mach-Zehnder interferogram but the LCPDI interferogram remained unchanged as can be seen in Figure 6 (c) and (d). A 10 mG acceleration at 600 Hz and a 6 G acceleration caused by a mallet strike also washed out the Mach-Zehnder without affecting the LCPDI. A 30 G strike disrupted the LCPDI slightly, but stability was quickly recovered. This shows that the LCPDI is less sensitive to vibration that the Mach-Zehnder. This is because the Mach-Zehnder object and reference beams traveled different paths, and the optical mounts in each path vibrated with respect to each other. This does not occur in the common-path LCPDI.

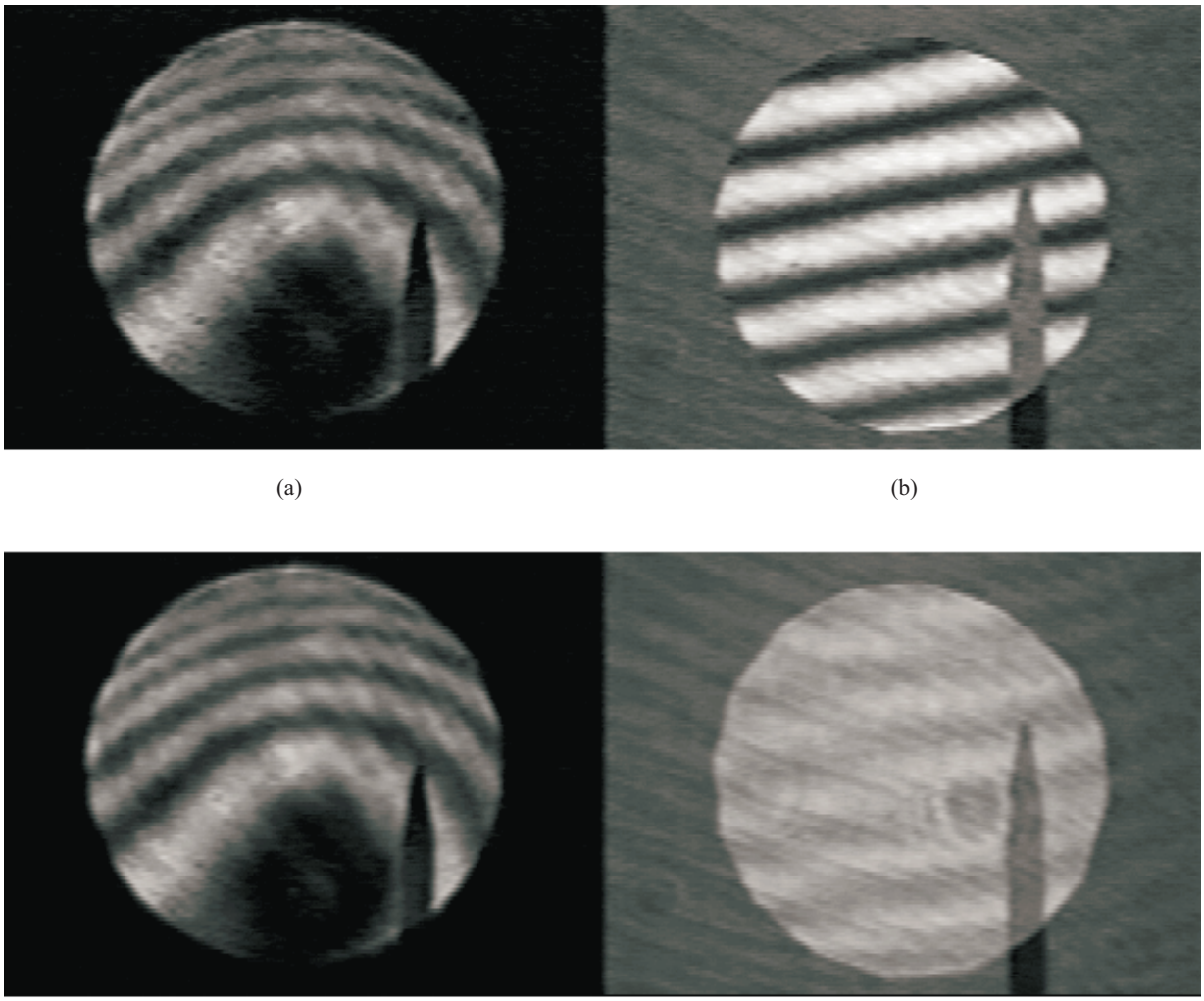

(a) (b)

(c) (d)

Fig. 6. Effect of vibration on LCPDI and Mach-Zehnder interferograms. a) LCPDI, no vibration. b) M-Z, no vibration, c) LCPDI, vibration, M-Z, vibration.

3.0 Conclusions

A liquid crystal point diffraction interferometer was compared directly to a Mach-Zehnder interferometer by making simultaneous temperature measurements with both. A silicone oil filled chamber was used as the test object. The top surface was held at a constant temperature and the bottom surface was set to several different temperatures. Differences between the various temperature distributions and the isothermal distribution were measured with both interferometers and compared. Very good general agreement was shown between the two interferometers, with measured vertical thermal gradients agreeing to within 3.6% except for two cases where more than 4 hours elapsed between the at-condition measurement and the isothermal reference measurement. Both interferometers also measured nominally flat horizontal temperature

distributions, but in each case the LCPDI measurement was nearer to the expected zero gradient. The LCPDI data was slightly noisier than the Mach-Zehnder, but was shown to be substantially more robust than the Mach-Zehnder in the presence of vibration. This robustness is a consequence of the LCPDI's common-path design.

References

[1] Mercer CR, Creath K. Liquid crystal point diffraction interferometer for wavefront measurement. Applied Optics, Vol. 35, No. 10, pp 1633-1642, 1996.

[2] Mercer CR, Rashidnia N, Creath K. High data density temperature measurement for steady-state flows. Experiments in Fluids, Vol. 21, No. 1, pp 11-16, 1996.

[3] Hariharan P. *Optical Interferometry*. Academic Press, 1987.

[4] Hariharan P, Oreb BF, Eiju T. Digital phase-shifting interferometry: a simple error-compensating phase calculation algorithm. Applied Optics, Vol. 26, No. 13, pp 2504-2506, 1987.

[5] Vest CM. *Holographic Interferometry*. John Wiley & Sons, 1979.

REPORT DOCUMENTATION PAGE

Form Approved
OMB No. 0704-0188

1. AGENCY USE ONLY (*Leave blank*)	2. REPORT DATE	3. REPORT TYPE AND DATES COVERED
	September 1999	Technical Memorandum

4. TITLE AND SUBTITLE

Common-Path Phase-Stepped Interferometer for Fluid Measurements

5. FUNDING NUMBERS

WU–274–00–00–00

6. AUTHOR(S)

Carolyn R. Mercer and Nasser Rashidnia

7. PERFORMING ORGANIZATION NAME(S) AND ADDRESS(ES)

National Aeronautics and Space Administration
John H. Glenn Research Center at Lewis Field
Cleveland, Ohio 44135–3191

8. PERFORMING ORGANIZATION REPORT NUMBER

E–11449

9. SPONSORING/MONITORING AGENCY NAME(S) AND ADDRESS(ES)

National Aeronautics and Space Administration
Washington, DC 20546–0001

10. SPONSORING/MONITORING AGENCY REPORT NUMBER

NASA TM—1999-208837

11. SUPPLEMENTARY NOTES

Prepared for the eighth International Symposium on Flow Visualization sponsored by the International Flow Visualization Society, Sorrento, Italy, September 1–4, 1998. Carolyn Mercer, NASA Glenn Research Center and Nasser Rashidnia, National Center for Microgravity Research, Glenn Research Center, Cleveland, Ohio 44135–3191. Responsible person, Carolyn R. Mercer, organization code 5520, (216) 433–3411.

12a. DISTRIBUTION/AVAILABILITY STATEMENT

Unclassified - Unlimited
Subject Categories: 35 and 74 Distribution: Nonstandard

This publication is available from the NASA Center for AeroSpace Information, (301) 621–0390.

12b. DISTRIBUTION CODE

13. ABSTRACT ***(Maximum 200 words)***

The liquid-crystal point-diffraction interferometer is a new phase-stepped, common-path interferometer. A microsphere in a liquid crystal layer is used to locally generate a reference beam and phase-shift the object beam. The result is an interferometer that provides quantitative, high-density data in relatively high vibration environments. This paper describes a comparison between the liquid-crystal PDI and a phase-stepped Mach-Zehnder interferometer. Both were used to simultaneously measure temperature distributions in an oil bath. Very good agreement between the data from both interferometers is shown, and the common-path interferometer is shown to be more robust in the presence of vibrations.

14. SUBJECT TERMS

Interferometry; Instrumentation; Lasers; Optics

15. NUMBER OF PAGES

15

16. PRICE CODE

A03

17. SECURITY CLASSIFICATION OF REPORT	18. SECURITY CLASSIFICATION OF THIS PAGE	19. SECURITY CLASSIFICATION OF ABSTRACT	20. LIMITATION OF ABSTRACT
Unclassified	Unclassified	Unclassified	